Rotational transitions of SO, SiO, and SiS excited by a discharge in a supersonic molecular beam: Vibrational temperatures, Dunham coefficients, Born–Oppenheimer breakdown, and hyperfine structure

M. Eugenia Sanz,[a] Michael C. McCarthy, and Patrick Thaddeus
Harvard-Smithsonian Center for Astrophysics, Cambridge, Massachusetts 02138 and Division of Engineering and Applied Sciences, Harvard University, Cambridge, Massachusetts 02138

(Received 11 September 2002; accepted 31 July 2003)

Fourier transform microwave spectroscopy has been used to investigate vibrational excitation and relaxation of diatomic molecules produced by an electric discharge in the throat of a supersonic nozzle. Rotational transitions of SO, SiO, and SiS, in vibrational states up to $v=33$ for $^{32}S^{16}O$, $v=45$ for $^{28}Si^{16}O$, and $v=51$ for $^{28}Si^{32}S$ in their ground electronic states have been detected. The isotopic species $^{33}S^{16}O$, $^{34}S^{16}O$, $^{29}Si^{16}O$, $^{28}Si^{18}O$, $^{29}Si^{32}S$, and $^{28}Si^{34}S$ have also been observed in highly excited vibrational states. Microwave transitions include up to $v=22$ for the second lowest excited electronic state $b\,^1\Sigma^+$ of SO ($\sim$10 510 cm^{-1} above ground) have also been detected. Effective vibrational temperatures have been derived for each species, and a general model is proposed to qualitatively explain the observations. Vibrational excitation is caused by inelastic collisions with the hot electrons produced in the discharge. The subsequent vibrational populations are largely determined by vibration–vibration energy transfer via molecule–molecule binary collisions. Two regions can be inferred from the data: one characterized by a temperature of around 1000 K and a second region with a temperature of several thousand degrees Kelvin. Improved Dunham coefficients and correction terms for the breakdown of the Born–Oppenheimer approximation have been determined for $b\,^1\Sigma^+$ SO, $X\,^1\Sigma^+$ SiO, and $X\,^1\Sigma^+$ SiS. Nuclear spin-rotation hyperfine structure for the ^{29}Si isotopic species of SiO and SiS has been observed in all highly excited vibrational states. © *2003 American Institute of Physics.*
[DOI: 10.1063/1.1612481]

I. INTRODUCTION

Supersonic molecular beams are a powerful tool for the study of transient species which can be produced efficiently in the throat of a nozzle and then studied by various spectroscopic techniques downstream in the collision-free region of the expansion. Because of its high sensitivity and resolution, Fourier transform microwave (FTM) spectroscopy has become one of the most widely used techniques to detect the rotational spectra of molecular systems such as weakly bound complexes,[1,2] refractory metal halides,[3] reactive carbon chains and rings,[4] and protonated molecular ions.[5,6] In this laboratory, molecular beam FTM spectroscopy together with electric discharges has been used to study nearly 100 new reactive molecules of astrophysical interest[4] during the past six years. In the course of these investigations, rotational satellite transitions from excited vibrational states of several new species have also been detected, some accidentally. The second lowest-frequency bending mode of SiC_4, for example, was recently observed,[7] as well as the second lowest-frequency bending vibration and the two highest-frequency stretching modes of SiC_2S.[8]

To better understand the vibrational excitation and relaxation processes in our molecular beam discharge, we have undertaken a systematic study of the rotational spectra of several diatomic and small polyatomic molecules. The polyatomic data will be described elsewhere.[9] Here, we report the results for three diatomics: SO, SiO, and SiS. These molecules were chosen because they are produced in fairly high abundance in the adiabatic expansion after the application of dc electric discharges to gas mixtures of the right precursor gases. Partly because of their astrophysical importance, SO, SiO, and SiS have been widely studied using a number of spectroscopic techniques and their molecular constants are known to high accuracy, making identification of their excited vibrational states fairly straightforward.

The effect of electric discharges in vibrational excitation, relaxation, and energy transfer of diatomic molecules has been the subject of numerous studies,[10] especially so because of the importance of these processes for the operation of CO lasers,[11] where the population inversion depends on the vibrational distribution of the diatomic molecules after excitation in a discharge. It is also of interest for plasma diagnosis (see, for example, Ref. 12), since plasma properties can be estimated from molecular emission lines if the vibrational distribution in the ground and excited electronic states is known, and in combustion processes, for which it has been suggested that vibrationally excited species produced in the

[a]Current address: Departamento de Química Física, Facultad de Ciencias, Universidad de Valladolid, Prado de la Magdalena, s/n, 47005 Valladolid, Spain. Electronic mail: msanz@cfa.harvard.edu; mesanz@qf.uva.es

electric discharge significantly contribute to promotion of combustion mechanisms.[13]

Vibrational relaxation of diatomics in molecular beams has been investigated by electric resonance spectroscopy[14,15] and laser-induced fluorescence.[16,17] In these studies, excited vibrational states of several alkali halides and iodine seeded in beams of different gases (monoatomic, diatomic, or polyatomic molecules) were observed, but only up to $v \leqslant 5$ in the electronic ground state. These studies covered a wide range of experimental conditions, and, although restricted to the lowest-lying vibrational levels, they showed that vibrational relaxation in supersonic expansions is dominated by collisions with the diluent gas, and is sensitive to source pressure and temperature.

There have been few investigations of vibrational distributions in supersonic beams excited by an electric discharge. In one such study, vibrationally excited NO (up to $v=18$) has been investigated by means of a TOF-REMPI experiment.[18,19] The vibrational temperature was found to be highly dependent on the stagnation pressure; for a pressure of 3 bar (2.25 kTorr), a vibrational temperature of 6700 ± 700 K for $6<v<18$ was calculated—very similar, as it will be seen, to the temperatures derived here.

In this paper we present measurements of highly excited vibrational states ($v>30$) of SO, SiO, and SiS in a dc electric discharge molecular beam source under various experimental conditions. A qualitative model for the processes involved in vibrational excitation and relaxation is proposed. Inelastic collisions with the electrons produced in the discharge efficiently couple much of the electron kinetic energy, characterized by temperatures of the order of 10^4 K, into vibrational excitation. Vibrational relaxation occurs mainly via vibration–vibration (VV) energy transfer, which redistributes the energy up and down the vibrational ladder, giving rise to two distinct regions: one for the lowest-lying vibrational levels, at temperatures around 1000 K, and another region for higher vibrational states where temperatures of several thousand degrees K are achieved.

The detection of very highly excited vibrational states for the three diatomics here allowed us to derive new spectroscopic data for SiO, SiS, and the second lowest-lying excited electronic state ($b\,^1\Sigma^+$) of SO. Dunham-type expansions were employed to fit the measured transitions, and new and improved Dunham coefficients together with Born–Oppenheimer breakdown correction terms were obtained. The high resolution and sensitivity of molecular beam FTM spectroscopy enabled us to observe the spin-rotation hyperfine structure (hfs) for highly excited vibrational states of the ^{29}Si isotopomers of SiO and SiS. Spin-rotation constants were derived and their vibrational dependence determined.

II. EXPERIMENT

Rotational spectra have been measured with a molecular beam FTM spectrometer described elsewhere;[20,21] this instrument currently operates in the 5–40 GHz frequency range and incorporates a pulsed-discharge nozzle whose geometry and electrical characteristics have been adjusted to produce small reactive molecules in high abundance. As shown in Fig. 1, the nozzle consists of a commercial solenoid valve with a 1 mm diameter orifice and alternating layers of copper electrodes and Teflon insulators, each a few millimeters thick. It is located in the center of one of the large mirrors of the Fabry–Pérot resonator of the spectrometer.

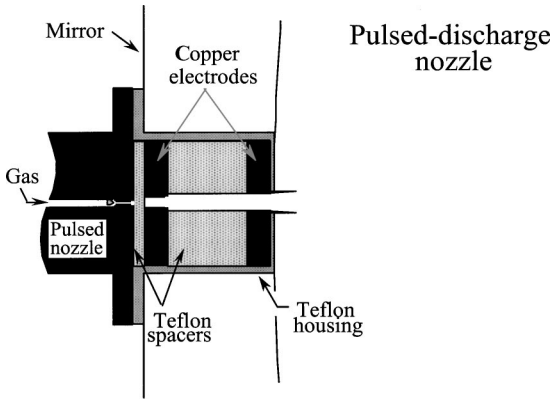

FIG. 1. Cross section of the pulsed-discharge nozzle.

The supersonic beam is produced by the adiabatic expansion of various precursor gases diluted in either He or Ne at backing pressures of typically 2.5 kTorr (3.3 atm, $Pd = 250$ Torr cm). As the pulsed beam expands, a low-current electric discharge is produced synchronously with the gas pulse in the throat of the nozzle by applying a dc voltage to one of the copper electrodes. After the gas pulse has expanded to fill the Fabry–Pérot cavity of the spectrometer, the molecules under study are polarized by a short (1 μs) microwave pulse, which is coupled into the cavity by a small antenna. Molecular emission as a function of time is subsequently detected with a superheterodyne receiver and Fourier transformed to obtain the power spectrum.

Vibrational cooling in a supersonic nozzle depends on a number of experimental parameters, including backing pressure, buffer gas, discharge current, and the geometry of the nozzle, so care was taken to use a fairly uniform set of experimental conditions in our experiments. The same rotational transition has been measured for each vibrational state; the cavity Q and amplifier gains are constant to about 15% over the frequency range of the vibrational shifts, which are generally less than 10 GHz. Care was also taken to use the same microwave power for each measurement, and relative intensities were derived from several measurements for each vibrational state (averaging peak heights). Finally, it should be emphasized as a check that (i) the intensity data for nearly all of the species studied here are well-described by a Boltzmann distribution implying that systematic intensity uncertainties are small (assuming that the dipole dependence of the vibrational ladder is either known or assumed to be constant with v); (ii) similar vibrational temperatures were derived for the normal and less abundant isotopic species; and (iii) the vibrational temperature of SiO measured here ($\sim$9500 K for the parent isotopic species) agrees (surprisingly) well with that measured in our free-space cell previously ($\sim$10 000 K).[22]

All three diatomic molecules have been produced with discharge voltages that optimize the intensity of their vibra-

TABLE I. Summary of present laboratory measurements.

Molecule	Precursor gases	Carrier gases	Concentration (%)	Voltage (V)	Frequency band (GHz)	Vibrational level
$X\,^3\Sigma^-$ SO	OCS	Ne	0.15	1100	29–42	33
$X\,^3\Sigma^-$ SO	SO_2	He or Ne	0.15	500,600,1000,1500	29–42	30
$b\,^1\Sigma^+$ SO	SO_2	Ne	0.15	1300	29–42	22
$X\,^1\Sigma^+$ SiO	SiH_4/O_2[a]	Ne	0.15/0.4	1100	28–44	46
$X\,^1\Sigma^+$ SiS	SiH_4/CS_2[a]	Ne	0.2/0.05	1400	17–37	51

[a]Because SiH_4 is spontaneously flammable in air, separate gaseous samples of 2% SiH_4 in Ar and 1.5% O_2 in Ne or 1% CS_2 in Ne were further diluted with Ne and mixed in the gas input line just before the discharge nozzle.

tional ground-state lines. The duration of the gas pulse employed was typically 350–400 μs, which corresponds to flow rates of 15–25 sccm at the 6 Hz repetition rate of the nozzle, yielding a typical background pressure in the vacuum chamber of 5×10^{-6} Torr. Typical rotational temperatures in our free expansion are 3 K. All lines exhibit Doppler splitting into two well-resolved components, owing to the coaxial alignment of the molecular beam with the direction of propagation of the microwave radiation. Experimental conditions used to observe the three diatomic molecules (precursor gases and voltages employed) are given in Table I.

III. RESULTS

A. Analysis of the rotational spectra

1. Sulfur monoxide

The large spin–spin interaction ($\lambda=158$ GHz[23]) in SO brings several of its rotational transitions within the band of our spectrometer, including the intense $N_J=0_1\rightarrow1_0$ transition at 30 GHz. This radical has been previously observed using molecular beam FTM spectroscopy by at least three other groups, but only excited vibrational states to $v=2$ in the $X\,^3\Sigma^-$ electronic state have been previously reported.[24–26] By using other techniques, such as millimeter-wave spectroscopy in combination with dc electric discharges or UV-laser photolysis, SO has been observed in higher excited vibrational states, ranging up to $v=17$, $v=13$, and $v=11$ for the $X\,^3\Sigma^-$, $a\,^1\Delta$, and $b\,^1\Sigma^+$ electronic states, respectively. From these measurements Dunham coefficients were derived for each electronic state.[23]

During an unsuccessful search for OCS^+, progressions of the $N_J=0_1\rightarrow1_0$ rotational transition of ^{32}SO and ^{34}SO in even higher vibrational levels of the $X\,^3\Sigma^-$ state were initially observed here in a discharge of dilute OCS in Ne (see Table I). These were assigned fairly easily by extrapolation from previous work[23,27] up to $v=33$, because rotational lines from successive vibrational levels are separated by a nearly constant frequency interval [see Table I of Supplementary Material (SM), deposited in the Electronic Physics Auxiliary Publication Service (EPAPS) of the American Institute of Physics[28]].

A discharge of SO_2 was found to give more intense SO signals, so this precursor gas was employed for the detection of the weaker lines of the ^{33}S isotopic species (0.76% natural abundance) in the ground electronic state. The $J=1\rightarrow0$ microwave transition of $^{32}S^{16}O$ in the second low-lying metastable electronic state $b\,^1\Sigma^+$, at $\sim10\,510$ cm^{-1} above ground,[23] was also observed. On the basis of the constants provided in Refs. 23 and 27, vibrational excited states up to $v=8$ for the $X\,^3\Sigma^-$ state of ^{33}SO (Table II of SM[28]) and $v=22$ for the $b\,^1\Sigma^+$ state of ^{32}SO (Table III of SM[28]) were identified—a significant extension of previous measurements.

The highest observed vibrational level for ^{32}SO in the ground electronic state, $v=33$, lies about 3.8 eV above ground, equivalent in temperature to 44 120 K, almost three-quarters of the dissociation limit [$D_e=5.359$ eV$=62\,189$ K (Ref. 29), and references therein]. The highest vibrational level measured for the $b\,^1\Sigma^+$ state has a comparable energy of $\sim$44 150 K above the ground electronic state. No measurements of SO in the first excited electronic state $a\,^1\Delta$ were possible since its lowest rotational transition at 127.8 GHz lies well above the frequency range of our spectrometer.

Extensive rotational and vibrational data are available for the SO radical in the ground electronic state,[23,27] including molecular constants and the Born–Oppenheimer breakdown correction terms, which have been derived via global fits of all isotopic species incorporating large numbers of SO transitions. It is mainly because of this large body of work that no attempt is made here to rederive spectroscopic contants or Dunham coefficients for SO on the basis of our new data. Our results, however, may still be of some value. In combination with previously published frequencies, it should be possible to determine additional higher-order constants for the normal species because frequencies of rotational transitions determined from FTM spectroscopy are generally accurate to a few kHz—about a factor of 10 more precise than most previously reported measurements—and because the present data probe the SO potential at twofold higher vibrational energies than that probed previously by UV-laser photolysis of Cl_2SO.[27]

For the $b\,^1\Sigma^+$ electronic state, the Dunham coefficients Y_{ij} have been reported for ^{32}SO (Refs. 23, 30) and ^{34}SO,[30] but no global fit has been undertaken previously. Therefore, the new rotational transitions for the $b\,^1\Sigma^+$ state measured here were fit together with those previously measured[23,30] to a Dunham-type expansion using LeRoy's program DSPARFIT.[31] This program simultaneously fits data from all isotopic species to determine the Dunham coefficients Y_{ij} and the Born–Oppenheimer breakdown correction terms δ_{ij} of a selected reference isotopomer (usually the most abundant one, for which more experimental data are generally available), using the expansion:[31]

TABLE II. Dunham Y_{ij} coefficients of SO in the $b\ ^1\Sigma^+$ electronic state (in MHz).

Y_{ij}	$^{32}S^{16}O$	$^{34}S^{16}O$	Bogey *et al.* ($^{32}S^{16}O$)[a]	Yamamoto *et al.* ($^{34}S^{16}O$)[b]
Y_{01}	21 064.977 1(15)[c]	20 652.312 6(22)	21 064.978 5(14)	20 652.320(20)
Y_{11}	−191.048 6(18)	−185.461 6(18)	−191.051 6(18)	−185.468(18)
$Y_{21}\times10^2$	−5.022(74)	−4.827(71)	−4.831(82)	[−4.76][d]
$Y_{31}\times10^3$	−5.88(13)	−5.60(12)	−6.43(17)	[−5.68]
$Y_{41}\times10^4$	−2.66(11)	−2.51(10)	−1.87(16)	[−2.44]
$Y_{51}\times10^6$	1.61(43)	1.50(40)	−3.92(56)	⋯
$Y_{61}\times10^7$	−1.356(65)	−1.252(60)	⋯	⋯
$Y_{02}\times10^2$	−3.641 67(50)	−3.500 37(48)	−3.642 43(33)	−3.504(16)
$Y_{12}\times10^4$	−1.334(17)	−1.270(16)	−1.307(17)	−1.0(15)
$Y_{22}\times10^6$	−2.36(34)	−2.22(32)	−3.21(45)	[−3.8]
$Y_{32}\times10^7$	−2.54(19)	−2.37(17)	−1.88(34)	⋯
$Y_{03}\times10^8$	−2.06(61)	−1.95(57)	−1.23(37)	⋯
δ_{01}^S	0.847(32)	⋯	⋯	⋯
r_e (Å)	1.500 109 6(5)	1.500 107 9(5)	⋯	⋯

[a]Reference 23.
[b]Reference 30.
[c]Numbers in parentheses are 95% confidence limits in units of the last digit except those for r_e, that are one standard deviation in units of the last digit. Dimensionless standard error $\sigma=0.8$.
[d]Parameters in square brackets calculated from the corresponding values of $^{32}S^{16}O$ in Ref. 30 and kept fixed in the fit.

$$E_\alpha(v,J)=\sum_{(i,j)\neq(0,0)}\left(\frac{\mu_1}{\mu_\alpha}\right)^{j+i/2}Y_{ij}^1(v+1/2)^i[J(J+1)]^j+\sum_{(i,j)\geqslant(0,0)}\left(\frac{\mu_1}{\mu_\alpha}\right)^{j+i/2}\left\{\left(\frac{M_A^\alpha-M_A^1}{M_A^\alpha}\right)\delta_{ij}^A+\left(\frac{M_B^\alpha-M_B^1}{M_B^\alpha}\right)\delta_{ij}^B\right\}(v+1/2)^i[J(J+1)]^j, \quad (1)$$

where α refers to a given isotopic species and 1 indicates the reference isotopomer. The Dunham parameters for isotopic species other than the reference species are readily calculated from the relation:[31,32]

$$Y_{ij}^\alpha=\left[Y_{ij}^1+\left(\frac{M_A^\alpha-M_A^1}{M_A^\alpha}\right)\delta_{ij}^A+\left(\frac{M_B^\alpha-M_B^1}{M_B^\alpha}\right)\delta_{ij}^B\right]\left(\frac{\mu_1}{\mu_\alpha}\right)^{j+i/2}. \quad (2)$$

Additional details of the fit, the merits of using this type of expansion, and the relation of the Y_{ij} terms to the mass-independent parameters U_{ij} are discussed in Refs. 31 and 32.

The fit for the $b\ ^1\Sigma^+$ state of SO includes all of the measured rotational transitions, with assigned uncertainties of 2 kHz (present work), 20 kHz (Ref. 30), and 50 kHz (Ref. 23). The resulting Dunham coefficients are given in Table II, together with the values of the equilibrium distances of both isotopic species, derived from the standard relation

$$r_e=\left(\frac{h}{8\pi^2\mu Y_{01}}\right)^{1/2}, \quad (3)$$

where μ is the reduced mass. Two new parameters, Y_{61} and the δ_{01}^S correction term for the sulfur nucleus, were required in the global fit to obtain an rms comparable to the estimated uncertainty of the measurements. Correction terms for the breakdown of the Born–Oppenheimer approximation for the oxygen atom could not be determined since there are presently no experimental data for its rare isotopic species.

2. Silicon monoxide

The microwave and infrared spectrum of SiO has been extensively studied by a number of techniques.[22,33–37] Mollaaghababa *et al.*[22] detected rotational transitions in excited vibrational states up to $v=40$ of the $^1\Sigma^+$ electronic ground state by millimeter wave spectroscopy in a glow discharge free-space cell. The infrared emission spectrum of the parent isotopic species has been measured up to $v=13\rightarrow12$,[36] and refined Dunham coefficients were derived from a global fit of the available infrared, microwave, and millimeter-wave data. Data on the Si atom were insensitive to the breakdown of the Born–Oppenheimer approximation; that plus the lack of isotopic information on the oxygen atom prevented a determination of the Born–Oppenheimer breakdown correction terms. The microwave spectrum of the ^{18}O isotopic species in the ground vibrational state was, however, later reported by Cho and Saito.[37]

Investigation of vibrationally excited SiO was further stimulated by the prospects of improving its spectroscopic contants and determining the Born–Oppenheimer correction terms. The SiO molecule was produced in our molecular beam under the conditions summarized in Table I. In its vibrational ground state, only the lowest rotational transition at 43 GHz lies within the present frequency range of our spectrometer. This transition in vibrational excited states up to $v=45$, where its frequency is only 30 GHz (see Table IV of SM[28]), was detected for the normal isotopic species. Rotational transitions up to $v=43$ of $^{28}Si^{18}O$ (Table IV of SM[28]) were also detected using $^{18}O_2$ as a precursor gas under the same experimental conditions and the SiH_4/O_2 ratio employed for the other isotopomers. The ^{29}Si isotopic species was observed in natural abundance in states as high as $v=26$ (Table V of SM[28]). All transitions of the ^{29}Si species exhibited hfs from the spin–rotation interaction of the ^{29}Si nucleus with the weak magnetic field generated by the rotation of the molecule (see Fig. 2). In spite of the high spectral

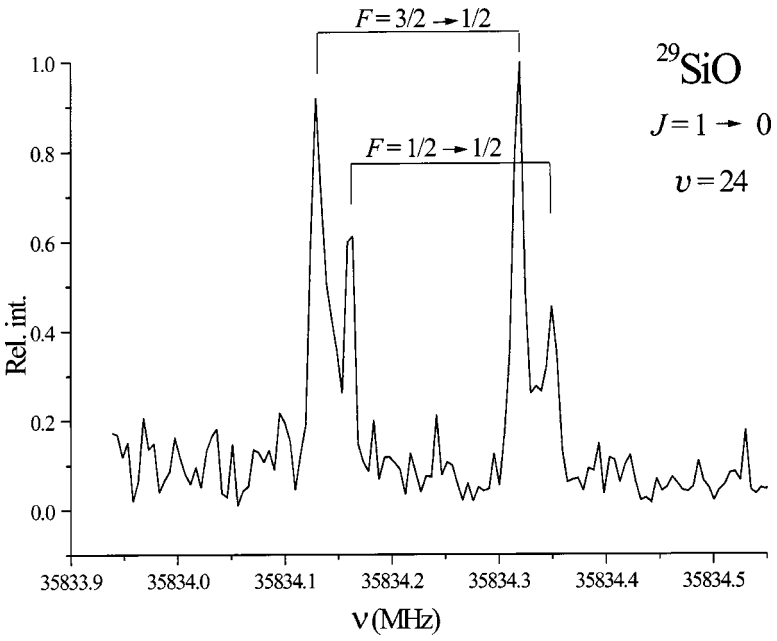

FIG. 2. The $J=1\rightarrow 0$ rotational transition in the $v=24$ excited vibrational state of ^{29}SiO, showing the ^{29}Si spin–rotation hfs. Experimental conditions: the spectrum was taken after integration of 23 min and 1360 cycles.

resolution, no vibrational dependence of the nuclear spin–rotation coupling constant C_I could be discerned. The hyperfine components of all vibrational states were simultaneously fit with Pickett's program[38] to determine the rotational constant B_v of each vibrational state and a common (to all vibrational states) spin–rotation coupling constant $C_I=-0.021\,40(34)$ MHz (rms deviation $\sigma=0.9$ kHz). The B_v rotational constants determined from the fit agree with the corresponding values derived from the Dunham parameters (Table III) to 0.0003% in the worst case.

The transitions measured here were also fit together with all previously reported data to the Dunham-type expansion of Eq. (1) by means of the DSPARFIT program described in Sec. III A 1.[31] The different data sets were assigned the following uncertainties: 100 kHz for the microwave data of Törring[33] and Manson *et al.*,[34] 20 kHz for that of Cho and Saito,[37] 30 kHz for that of Mollaaghababa,[22] and 2 kHz for the present FTM measurements. The infrared measurements[36] were kindly provided by Bernath with their corresponding uncertainties, and added to the fit. The ^{29}Si^{16}O line frequencies in the absence of hfs were calculated from the intensity-weighted average of the components and added to the fit as well. This global fit yields 18 Y_{ij} Dunham constants and the first information on the breakdown of the

TABLE III. Dunham Y_{ij} coefficients of SiO (in MHz).

Y_{ij}	^{28}Si^{16}O	^{29}Si^{16}O	^{30}Si^{16}O	^{28}Si^{18}O
Y_{10}	37 220 549.0(40)[a]	36 986 290.5(40)	36 766 797.5(39)	35 877 840.3(38)
Y_{20}	−179 107.1(14)	−176 859.7(14)	−174 766.8(14)	−166 417.9(13)
Y_{30}	182.58(18)	179.16(18)	175.99(18)	163.53(16)
Y_{40}	−0.332 9(74)	−0.324 6(72)	−0.317 0(70)	−0.287 4(64)
Y_{01}	21 787.478 6(11)	21 514.113 9(12)	21 259.545 4(14)	20 244.051 7(11)
Y_{11}	−151.030 63(66)	−148.196 87(65)	−145.574 10(63)	−135.269 03(59)
$Y_{21}\times 10^2$	7.328(13)	7.145(13)	6.977(13)	6.326(11)
$Y_{31}\times 10^4$	−3.16(11)	−3.06(11)	−2.97(11)	−2.627(94)
$Y_{41}\times 10^5$	−1.971(46)	−1.898(45)	−1.831(43)	−1.581(37)
$Y_{51}\times 10^7$	3.608(90)	3.452(86)	3.311(83)	2.790(70)
$Y_{61}\times 10^9$	−3.445(67)	−3.275(64)	−3.123(61)	−2.567(50)
$Y_{02}\times 10^2$	−2.984 58(44)	−2.910 15(43)	−2.841 68(42)	−2.576 66(38)
$Y_{12}\times 10^5$	−1.464(11)	−1.419(11)	−1.377(11)	−1.218(96)
$Y_{22}\times 10^7$	−5.043(94)	−4.855(90)	−4.685(87)	−4.045(75)
$Y_{32}\times 10^9$	−9.42(34)	−9.02(32)	−8.65(31)	−7.29(26)
$Y_{03}\times 10^9$	−4.20(94)	−4.04(90)	−3.90(87)	−3.67(75)
$Y_{04}\times 10^{13}$	4.34(68)	4.12(64)	3.93(61)	3.23(51)
$Y_{05}\times 10^{18}$	−6.0(16)	−5.6(15)	−5.3(14)	−4.1(11)
$\delta_{01}^{\mathrm{Si}}$	0.553(15)	⋯	⋯	⋯
δ_{01}^{O}	1.545 6(71)	⋯	⋯	⋯
$\delta_{11}^{\mathrm{O}}\times 10^3$	−8.69(30)	⋯	⋯	⋯
r_e (Å)	1.509 737 7(5)	1.509 736 9(5)	1.509 736 1(5)	1.509 731 7(5)

[a]Numbers in parentheses are 95% confidence limits in units of the last digit except those for r_e, that are one standard deviation in units of the last digit. Dimensionless standard error $\sigma=1.1$.

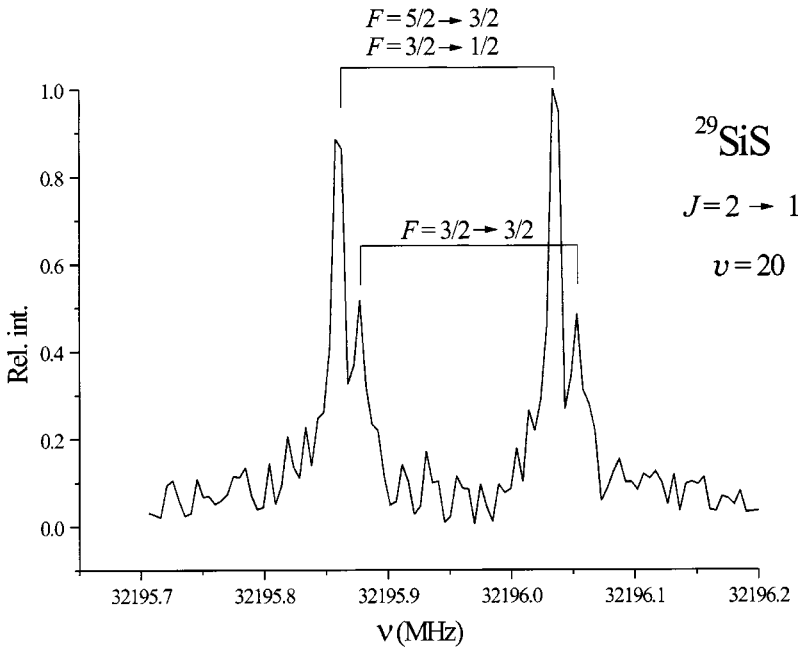

FIG. 3. The $J=2\rightarrow1$ rotational transition in the $v=20$ excited vibrational state of ^{29}SiS, showing the ^{29}Si spin–rotation hfs. Experimental conditions: the spectrum was taken after integration of 4 min and 225 cycles.

Born–Oppenheimer approximation on both the silicon and oxygen nuclei (Table III). Equilibrium distances r_e have also been derived from the Y_{01} [see Eq. (3)] for each isotopomer.

3. Silicon sulfide

SiS, isovalent with carbon monoxide and also an important astronomical molecule, is apparently a key starting point in the synthesis of silicon-containing molecules in the circumstellar shell of IRC+10216.[39,40] The infrared vibration–rotation spectrum of SiS has been detected by Bernath *et al.*,[41] who observed several vibrational bands of different isotopic species and derived a set of Dunham constants and correction terms for the breakdown of the Born–Oppenheimer approximation. The microwave spectrum of SiS has been reported previously only up to $v=4$ and $J=3\rightarrow2$.[42]

The two lowest-frequency rotational transitions of $X\,^1\Sigma^+$ SiS lie within the frequency range of our spectrometer. Under the conditions given in Table I, vibrationally excited SiS has been detected up to $v=51$ and spectra of three isotopic species, ^{28}Si^{32}S, ^{28}Si^{34}S, and ^{29}Si^{32}S, have been measured in natural abundance (see Tables VI and VII of SM[28]). All transitions of the ^{29}Si species exhibit spin–rotation hfs, similar to that of ^{29}SiO (see Fig. 3). There is again no evidence for vibrational dependence of the spin–rotation constant C_I. Hyperfine components from all vibrational states were fit simultaneously to yield B_v, D_v, and a common value of the C_I spin–rotation coupling constant using Pickett's program SPFIT.[38] The derived C_I is $-0.010\,39(21)$ MHz (rms deviation $\sigma=1.8$ kHz). The B_v rotational constants determined from the fit agree with the corresponding values derived from the Dunham parameters (Table IV) to 0.0006% in the worst case.

Our microwave measurements together with the infrared transitions[41] were included in a global fit to determine a new set of Dunham coefficients and the terms describing the breakdown of the Born–Oppenheimer approximation (see Table IV), using 2 kHz uncertainties for the microwave measurements and the stated uncertainties for the infrared data.[41] As before, unperturbed frequencies for ^{29}SiS were calculated from the intensity-weighted averages of the spin–rotation components. Three new Y_{i1} parameters have been determined (Table IV).

B. Vibrational populations

1. Silicon sulfide

The two lowest-J rotational transitions of SiS have been measured to $v=51$ under the experimental conditions shown in Table I, and effective vibrational temperatures were calculated as the inverse of the slope from linear fits of the Napierian logarithms of the observed intensities for each vibrational state relative to the vibrational ground state. No experimental data on the dependence of the dipole moment with v are available, but *ab initio* calculations[43] have yielded values for μ_e and the first coefficient of the power series expansion of the dipole moment in $(v+1/2)$. Using this dependence, the intensities of the rotational transitions of the excited vibrational states have been corrected for variations in the dipole moment. The plots of Fig. 4 seem to indicate the existence of two distinct vibrational temperatures: one at low v, with temperatures approximately in the range 1000–2000 K, and one at $v>6$ with temperatures in the 5000–6500 K interval (Table V).

The observations can be simply understood in terms of the competing energy transfer processes in the supersonic expansion following the discharge. These processes are exactly analogous to what occurs in CO lasers,[11] so only a brief description is provided here. Vibrational excitation of SiS is mainly caused by inelastic collisions with electrons whose kinetic temperature is in the vicinity of $\sim10\,000$ K.[44] Each molecule typically undergoes on the order of 10^2-10^3 binary

TABLE IV. Dunham Y_{ij} coefficients of SiS (in MHz).

Y_{ij}	$^{28}Si^{32}S$	$^{28}Si^{34}S$	$^{29}Si^{32}S$	$^{30}Si^{32}S$
Y_{10}	22 473 809.4(39)[a]	22 163 553.0(39)	22 266 120.4(39)	22 070 954.9(39)
Y_{20}	−77 533.3(23)	−77 407.3(23)	−76 106.9(23)	−74 778.6(23)
Y_{30}	31.43(52)	30.15(50)	30.57(50)	29.77(49)
Y_{40}	−0.240(37)	−0.227(35)	−0.231(36)	−0.223(35)
Y_{01}	9 099.536 21(36)	8 850.043 55(37)	8 932.140 99(37)	8 776.255 56(44)
Y_{11}	−44.163 33(20)	−42.359 40(19)	−42.950 22(20)	−41.830 69(19)
$Y_{21}\times10^{3}$	−1.198(36)	−1.134(34)	−1.155(35)	−1.115(33)
$Y_{31}\times10^{4}$	−2.080(27)	−1.940(26)	−1.986(26)	−1.900(25)
$Y_{41}\times10^{6}$	−3.48(10)	−3.205(93)	−3.295(96)	−3.126(91)
$Y_{51}\times10^{8}$	5.66(18)	5.14(16)	5.31(17)	4.99(16)
$Y_{61}\times10^{10}$	−5.16(12)	−4.62(10)	−4.79(11)	−4.46(10)
$Y_{02}\times10^{3}$	−5.965 00(90)	−5.642 37(85)	−5.747 54(86)	−5.548 66(83)
$Y_{12}\times10^{5}$	−0.586 8(27)	−0.547 4(25)	−0.560 2(25)	−0.536 1(24)
$Y_{22}\times10^{7}$	−0.840(64)	−0.773(59)	−0.794(61)	−0.754(58)
$Y_{03}\times10^{10}$	−1.54(48)	−1.41(44)	−1.45(45)	−1.38(43)
δ_{01}^{Si}	0.1958(40)	⋯	⋯	⋯
δ_{10}^{Si}	−392.(25)	⋯	⋯	⋯
δ_{01}^{S}	0.2766(23)	⋯	⋯	⋯
δ_{10}^{S}	69.(27)	⋯	⋯	⋯
r_e (Å)	1.929 321 4(6)	1.929 319 7(6)	1.929 320 1(6)	1.929 318 8(6)

[a]Numbers in parentheses are 95% confidence limits in units of the last digit except those for r_e, that are one standard deviation in units of the last digit. Dimensionless standard error $\sigma=0.7$.

collisions with other molecules (mainly with the atomic carrier gas) in a supersonic expansion,[45] which is insufficient to cool the high-frequency vibrational modes of a diatomic molecule to a temperature close to the translational temperature of the gas. However, vibration–vibration (VV) energy transfer involving collisions of two diatomic molecules plays an important role in the vibrational distribution. VV processes dominate vibration–translation (VT) transfer at low vibrational levels, causing a rapid redistribution of the energy by transferring population up the vibrational ladder, a redistribution which is aided by the anharmonicity of the potential as exothermic processes are preferred

$$2\,\mathrm{SiS}(v=n)\underset{k_2}{\overset{k_1}{\rightleftharpoons}}\mathrm{SiS}(v=n-1)+\mathrm{SiS}(v=n+1)+\Delta E.$$

Rate k_1 (exothermic) will be greater than rate k_2 (endothermic) by a factor $\exp(\Delta E/\mathrm{RT})$, which causes an asymmetrical distribution of the vibrational population. The few lowest vibrational levels are thereby cooled to a temperature considerably lower than that of the electrons (Treanor region).[46,47] As the vibrational quantum number increases, VV transfer becomes less efficient, resulting in a region with a relatively flat vibrational distribution, and a vibrational temperature which approaches the electron temperature (Plateau region). At even higher vibrational quantum numbers, for states approaching dissociation, VT energy exchange rates are dominant and the vibrational temperature rapidly decreases, so that a vibrational population distribution is established in approximate equilibrium with the local translational temperature (Boltzmann region).

The vibrational temperatures obtained from both of the observed transitions of SiS are very similar, which is evidence of rotational equilibrium (Table V), and the different isotopic species show similar vibrational temperatures as well. Since vibrational frequencies differ slightly for the several isotopomers, it is expected that VV energy transfer will tend to heat up the rare isotopic species (with lower stretching frequencies) with respect to the normal species. This tendency can be marginally inferred from the temperatures for SiS of Table V and Fig. 4 in the Plateau region.

2. Sulfur monoxide

Vibrational temperatures for $^{32}S^{16}O$ in its ground electronic state were derived from the relative intensities of the rotational transition $N_J=0_1\rightarrow1_0$ in vibrational levels up to $v=33$, in the same way as for SiS. The measurements were done with a discharge of OCS in Ne at a voltage of 1100 V ($I=24$ mA). The plot (see Fig. 5) marginally suggests the existence of two different vibrational temperatures: one at low v with $T\approx1785$ K, and one at $v>3$ with $T=10\,120\pm590$ K. This break, if real, is very similar to that observed for vibrationally excited SiO measured by millimeter-wave spectroscopy in a dc glow discharge of silane (SiH_4) and CO,[22] for which temperatures of 1000 K from $v=0$, 1 and 10 000 K from vibrational states up to $v=40$ were derived.

Because more intense signals of SO were observed when SO_2 was used as a precursor gas, additional experiments were carried out to detect vibrationally excited SO in a discharge of SO_2 in either Ne or He at various voltages. For each set of experimental conditions, vibrational temperatures were similar (see Table VI and Fig. 5), with the lowest vibrational levels having a vibrational temperature close to 1000 K, and the higher ones temperatures of several thousand degrees K. Vibrational temperatures in this latter region do not depend significantly on the carrier gas used (i.e., He or Ne), but they are apparently somewhat lower—by about 30%—than those obtained when the SO is produced in an OCS discharge (see Table VI). This discrepancy is plausibly the result of the production of CO in the OCS discharge, as discussed below.

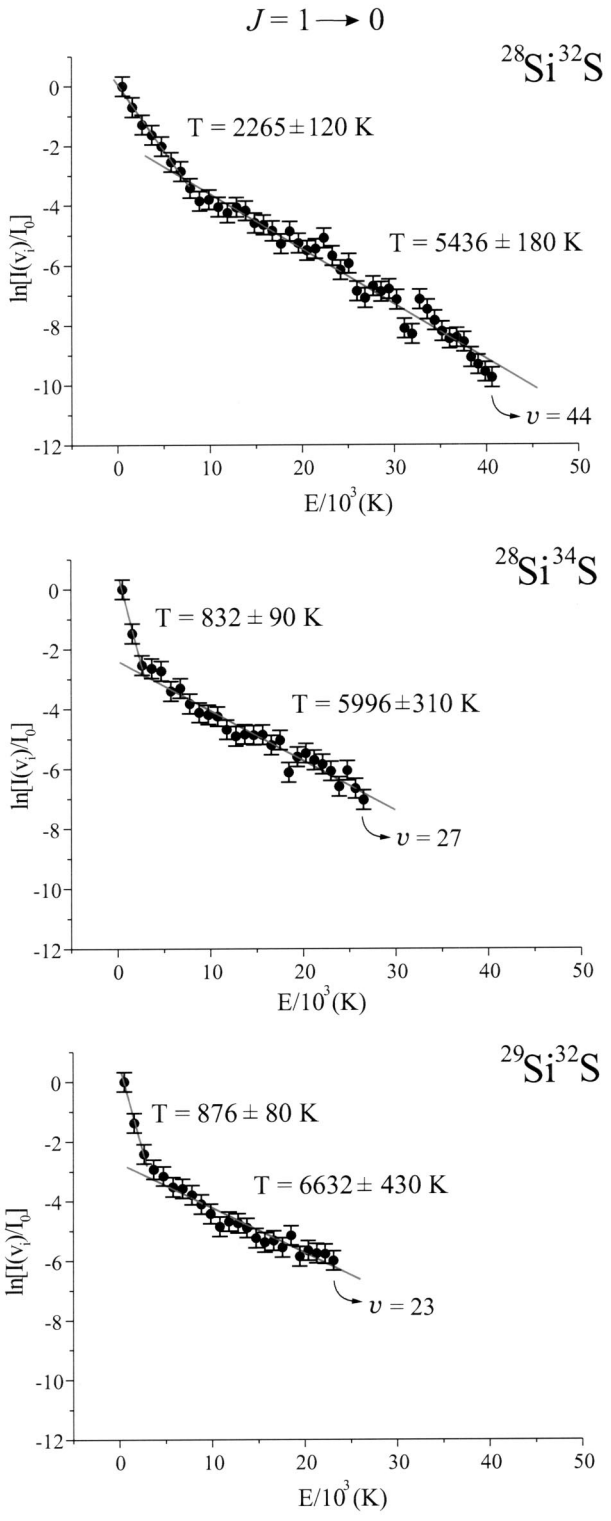

FIG. 4. Vibrational temperature diagram for the $J=1\rightarrow0$ transition of SiS. I_0 is the intensity of the $J=1\rightarrow0$ transition in the ground vibrational state. $I(v_i)$ is the intensity of the $J=1\rightarrow0$ transition in the different excited vibrational states. Error bars represent an estimated uncertainty of 15%.

From spectroscopic investigations of OCS in a glow discharge, it was concluded that at low average discharge currents ($I<50$ mA) the main reaction is decomposition of OCS to give CO+S.[48] As the current rises, however, there is an increase in the smaller concentrations of CS and SO which are formed via more complex secondary reaction paths. The chemical composition of the OCS discharge is determined almost entirely by the average current over a very wide range of experimental conditions.[48]

TABLE V. Effective vibrational temperatures for SiS and SiO.

	$J=1\rightarrow0$		$J=2\rightarrow1$	
Molecule	Treanor region	Plateau region	Treanor region	Plateau region
$^{28}Si^{32}S$	2265±120	5436±180	852±310	5305±110
$^{29}Si^{32}S$	876±80	6632±430	~800	5209±260
$^{28}Si^{34}S$	832±90	5996±310	1037±130	5338±240
$^{28}Si^{16}O$	···	9489±720	···	···
$^{29}Si^{16}O$	···	8028±1430	···	···
$^{28}Si^{18}O$	···	8141±350	···	···

The OCS discharge was studied by monitoring the intensity of the OCS and SO transitions in the ground vibrational state over a range of discharge currents. All measurements were performed with the same percentage of OCS in Ne as that used for the $X\ ^3\Sigma^-$ SO measurements. The other diatomics produced in the discharge, CO and CS, could not be monitored because their lowest rotational transitions lie above the frequency range of our spectrometer. Comparison of our results (see Fig. 6) with those of Ref. 48 suggests that our operating conditions correspond approximately to those of a glow discharge with $I<50$ mA, where the CO abundance is considerably higher than that of SO.

A significant amount of CO in our discharge means that VV energy transfer between CO and SO may be important. Theoretical models[47] predict different vibrational temperatures for a gas mixture of the two, with the VV energy transfer favored towards low vibrational states of the diatomics with higher vibrational frequency (yielding a lower vibrational temperature), and towards high vibrational levels of the molecule with lower vibrational frequency, as exothermic processes are more likely to occur. CO has a vibrational frequency $\omega_e=2170\ \mathrm{cm}^{-1}$,[29] while that of SO is $\omega_e=1149\ \mathrm{cm}^{-1}$.[29] Therefore, VV exchange between these two molecules will heat the SO vibrational ladder and cool down that of CO; a similar argument was proposed for SiO in a SiH_4+CO glow discharge.[22] The vibrational temperatures of the two diatomic molecules in the mixture (i.e., SiO and CO in one case, SO and CO in the other) depend on the difference in their vibrational frequencies. SiO has $\omega_e=1242\ \mathrm{cm}^{-1}$,[29] very close to that of SO, and, as expected, the vibrational temperatures derived for both diatomics when CO is present in either a pulsed discharge or a glow discharge are nearly the same.

Observations of the second lowest-lying electronic excited state $b\ ^1\Sigma^+$ of SO are possible in an electric discharge such as ours, because relaxation via electric dipole transitions to the first electronic excited state $a\ ^1\Delta$ or to the $^3\Sigma^-$ ground state are forbidden by the spin and orbital angular momentum selection rules. Since the time scale of our experiment is of the order of 1 ms, the $b\ ^1\Sigma^+$ state, which has a radiative lifetime of 5.7(8) ms,[49] does not relax. The experimental data of $b\ ^1\Sigma^+$ are quite scattered and the interpretation is ambiguous. Following what is suggested by the SiS data, two different vibrational temperatures could be derived

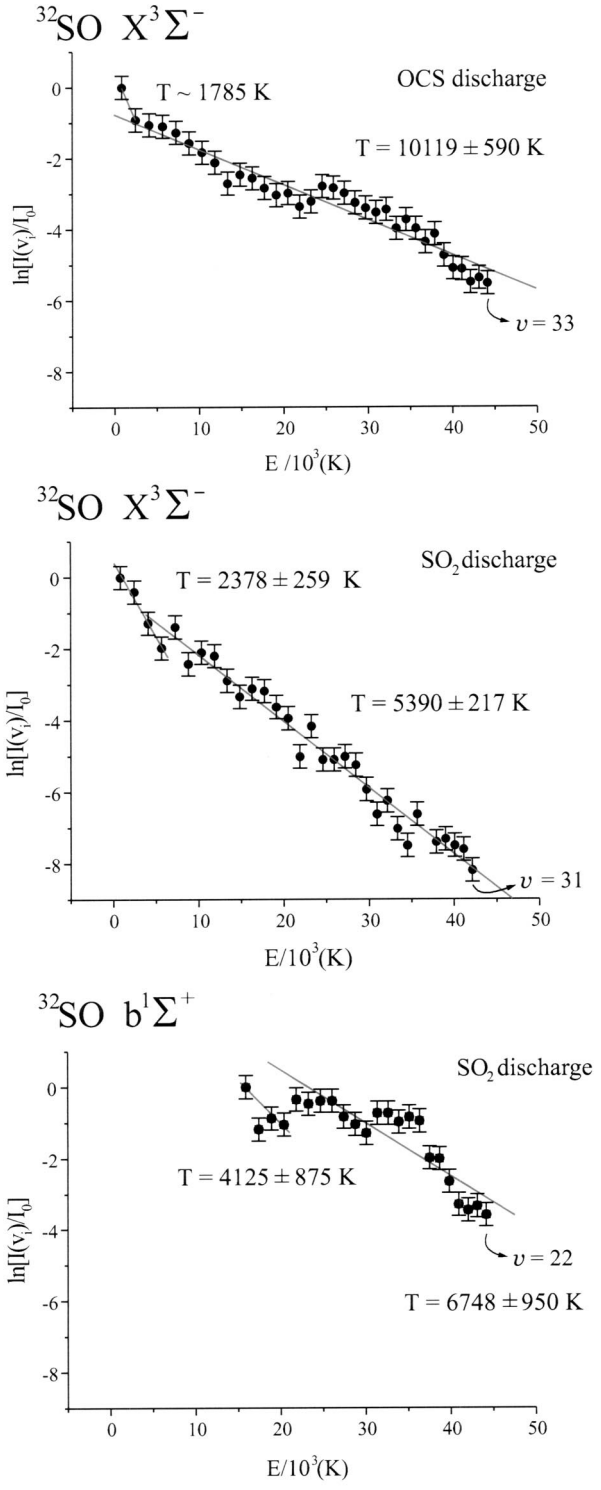

FIG. 5. Vibrational temperature diagrams for $X\,^3\Sigma^-$ SO in an OCS discharge (top), $X\,^3\Sigma^-$ SO in an SO_2 discharge (middle), and $b\,^1\Sigma^+$ SO in an SO_2 discharge (bottom). I_0 is the intensity of the $N_J=0_1\rightarrow1_0$ transition in the ground vibrational state. $I(v_i)$ is the intensity of the $N_J=0_1\rightarrow1_0$ transition in the different excited vibrational states. Error bars represent the estimated 15% uncertainty in the intensity measurements.

for the $b\,^1\Sigma^+$ state: 4125 ± 875 K, for the first three vibrational states, and 6748 ± 950 K for $v=4-22$ (Fig. 5). While this latter temperature is comparable to that determined for the $X\,^3\Sigma^-$ SO in an SO_2 discharge, the temperature of the lower vibrational excited states is about three times higher. If so, this might indicate less efficient VV exchange for the lowest vibrational levels in the excited electronic state, and less cooling than for the same vibrational levels of the ground electronic state. Further investigations on excited electronic states of diatomics will be necessary to test this tentative conclusion and to see if there is any relation between the vibrational temperature of the lower levels and the energy of the excited electronic state.

TABLE VI. Effective vibrational temperatures for $^{32}S^{16}O$ in the Plateau region from the $N'_{J'}\rightarrow N''_{J''}=0_1\rightarrow1_0$ transition. Temperatures were derived from intensity measurements of rotational lines in the $v=10$, 15, 20, 25, and 30 vibrational states in an SO_2 discharge.

Voltage (V)	Carrier gas He	Carrier gas Ne	Current in He (mA)	Current in Ne (mA)
500	⋯	7932±1320	⋯	1.3
600	5530±400	⋯	1.5	⋯
1000	6841±850	6625±1590	8.0	32.0
1500	7476±930	5077±650	23.0	60.0

To our knowledge, no experimental or theoretical data on the vibrational dependence of the SO electric dipole moment are available in the literature, and thus no attempt has been made to correct the vibrational temperatures of either the $X\,^3\Sigma^-$ and $b\,^1\Sigma^+$ electronic states for changes in the dipole moment with vibrational excitation. A dipole moment of $\mu=1.52(2)$ D for $v=0$ of $X\,^3\Sigma^-$ has been determined by microwave spectroscopy,[25] while for the $b\,^1\Sigma^+$ state only *ab initio* calculations exist.[50] These calculations predict a slight decrease in the dipole moment of the first two low-lying electronic states with respect to that of the ground electronic state, yielding μ_0 values of 1.51 D for $X\,^3\Sigma^-$, 1.45 D for $a\,^1\Delta$ (versus an experimental value of 1.34(5) D[51]), and 1.36 D for $b\,^1\Sigma^+$ SO. The degree of anharmonicity is larger for the $b\,^1\Sigma^+$ state ($\omega_e\chi_e=7.2$ cm^{-1} for $b\,^1\Sigma^+$ versus 5.6 cm^{-1} for $X\,^3\Sigma^-$ SO[29]), which will cause a slightly more pronounced decrease in the electric dipole moment as the vibrational quantum number increases—an effect which is not expected to significantly alter the vibrational temperatures.

Given the uncertainties in the data, the vibrational temperatures of SO in an SO_2 discharge are essentially the same as those found for SiS. The vibrational frequency of SiS [$\omega_e=749.6$ cm^{-1} (Ref. 29)] is only 2/3 of that of either SO or SiO, but still well above kT, with $T\approx300$ K the temperature behind the nozzle. Further research on diatomics with lower values of ω_e would be worthwhile to determine what vibrational temperatures are attained, and how VV and VT rates depend on vibrational frequency.

3. Silicon monoxide

Effective vibrational temperatures for SiO (Table V) were derived as for SiS and SO from the relative intensities of the rotational transitions in highly excited vibrational levels. Because rotational transitions from the lowest-lying vibrational states of $^{28}Si^{16}O$ are at 43 GHz—near the top of the frequency range of our spectrometer, where line intensities are least reliable—only excited vibrational states with $v>7$ were used to calculate the vibrational temperature. The

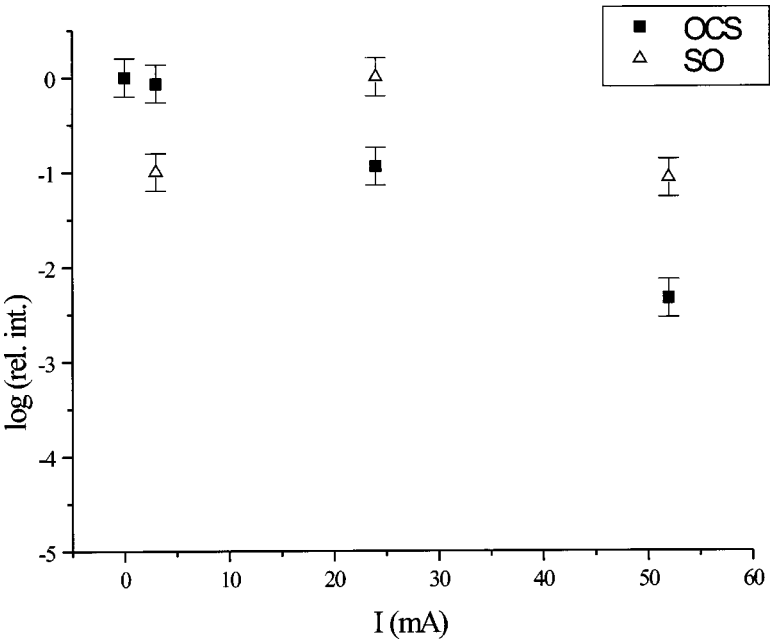

FIG. 6. Relative intensities of the $v=0$ $J=2\rightarrow1$ rotational transition of OCS and the $v=0$ $N_J=0_1\rightarrow1_0$ rotational transition of SO at different currents. Intensities of each rotational transition are normalized to their respective maximum values.

change of the electric dipole moment with v was determined from extrapolation of the dipole moments of the first four vibrational levels.[35]

The vibrational temperatures derived for the three isotopic species are very similar (Table V). They are all lower than those calculated for either SO or SiO in the presence of CO, but higher than those of SO in an SO_2 discharge. Because O_2 is used as a precursor gas, its abundance in our discharge is expected to be several orders of magnitude higher than that of SiO, and thus O_2-SiO collisions become important. The vibrational frequency of O_2 ($\omega_e=1580.2\ \mathrm{cm}^{-1}$[29]) exceeds that of SiO, so VV energy exchange between O_2 and SiO will tend to heat the SiO vibrational ladder in an analogous manner to that described above for SO in the presence of CO. O_2 is a nonpolar molecule, so that collision efficiency diminishes, and the difference between the vibrational frequencies of SiO and O_2 is smaller than that between SiO and CO. Consequently, the SiO vibrational temperature might be expected to be somewhat lower than that in the presence of CO—as observed.

IV. DISCUSSION

A. Born–Oppenheimer breakdown parameters

The Born–Oppenheimer breakdown correction terms have been determined for the two nuclei of the SiO and SiS diatomic molecules. To compare the results with those of other molecules, the δ_{ij} parameters obtained from LeRoy's program are transformed to the traditionally used dimensionless coefficients Δ_{ij} via the expression[31,32]

$$\Delta_{ij}^{\mathrm{A}}=\frac{-\delta_{ij}^{\mathrm{A}}M_A^1(\mu_1)^{j+i/2}}{U_{ij}m_e}, \tag{4}$$

where 1 indicates the reference isotopomer and

$$U_{ij}=(\mu_1)^{j+i/2}(Y_{ij}^1+\delta_{ij}^{\mathrm{A}}+\delta_{ij}^{\mathrm{B}}). \tag{5}$$

The calculated Δ_{ij}'s are shown in Table VII. Those of SiS are in reasonable agreement with previous values reported in the literature: $\Delta_{01}^{\mathrm{Si}}=-1.392(59)$ and $\Delta_{01}^{\mathrm{S}}=-1.870(65)$ from Ref. 52, and $\Delta_{01}^{\mathrm{Si}}=-1.203(52)$, $\Delta_{01}^{\mathrm{S}}=-1.944(58)$, $\Delta_{10}^{\mathrm{Si}}=0.929(22)$, and $\Delta_{10}^{\mathrm{S}}=-0.257(27)$ from Ref. 41. Δ_{01}^{O} of SiO is comparable to that of CO [$-2.0982(13)$[53]] or SO ($-2.7247(34)$[27]), while $\Delta_{01}^{\mathrm{Si}}$ of SiO is similar to that of SiS.

The Δ_{ij}'s include the adiabatic and nonadiabatic contributions to the Born–Oppenheimer approximation, as well as the Dunham correction. The last two terms can be individually calculated for Δ_{01} if the electric dipole moment and the rotational g_j factor of the diatomics are known:[53,54]

$$\begin{aligned}\Delta_{01}^{\mathrm{A}}&=(\Delta_{01}^{\mathrm{A}})^{\mathrm{ad}}+(\Delta_{01}^{\mathrm{A}})^{\mathrm{nonad}}+(\Delta_{01})^{\mathrm{Dunham}}\\&=(\Delta_{01}^{\mathrm{A}})^{\mathrm{ad}}+\frac{(\mu g_J)_B}{m_p}+\frac{\mu\Delta Y_{01}^{(\mathrm{D})}}{m_eB_e},\end{aligned} \tag{6}$$

where $(\mu g_J)_B$ is the isotopically independent value of μg_J referred to atom B, m_p is the mass of the proton, and $\Delta Y_{01}^{(\mathrm{D})}$ is the Dunham correction to Y_{01}. $(\Delta_{01}^{\mathrm{A}})^{\mathrm{ad}}$ is calculated from the values of the other Δ_{01}'s. The nonadiabatic contribution,

TABLE VII. Parameters related to the Born–Oppenheimer breakdown.

	SiO	SiS
$\Delta_{01}^{\mathrm{Si}}$	−1.294(35)	−1.097(22)
$(\Delta_{01}^{\mathrm{Si}})^{\mathrm{nonad}}$	−1.009 8(14)	−1.175 7(76)
$(\Delta_{01}^{\mathrm{Si}})^{\mathrm{ad}}$	−0.276(39)	0.084(32)
$\Delta_{01}^{\mathrm{Dunham}}$	−0.000 88(20)	−0.005 8(15)
$\Delta_{01}^{\mathrm{O/S}}$	−2.068 2(95)	−1.772(15)
$(\Delta_{01}^{\mathrm{O/S}})^{\mathrm{nonad}}$	−1.861 6(13)	−1.549 0(85)
$(\Delta_{01}^{\mathrm{O/S}})^{\mathrm{ad}}$	−0.198(13)	−0.217(25)
$\Delta_{10}^{\mathrm{Si}}$	⋯	0.890(57)
Δ_{10}^{S}	⋯	−0.179(70)
r_e (Å)	1.509 737 7(5)	1.929 321 4(6)
r^{BO} (Å)	1.509 665 0(17)	1.929 271 3(19)
r^{ad} (Å)	1.509 674 2(6)	1.929 273 3(7)

owing to the nonspherical distribution of the electrons in their shells, is, as expected, the most important one in SiO and SiS (see Table VII): it is one order of magnitude larger than the adiabatic term and two orders of magnitude larger than the Dunham correction.

Our results for SiS can be compared to those obtained by Tiemann *et al.*,[53] who evaluated the different contributions to Δ_{01} for a series of diatomic molecules. $(\Delta_{01})^{\text{nonad}}$ for both nuclei of SiS are the same as those given in Ref. 53 since they have been calculated using identical experimental parameters. Our different Dunham coefficients provide a $(\Delta_{01})^{\text{Dunham}}$ of SiS about half the value of Ref. 53 and a $(\Delta_{01}^{\text{Si}})^{\text{ad}}$ positive and remarkably different from the previous value of $-0.205(69)$.[53] $(\Delta_{01}^{\text{Si}})^{\text{ad}}$ can be estimated using the wobble-stretch theory:[53,55]

$$\Delta_{01}^{\text{ad}} \lesssim \frac{\mu^2 Y_{02} \Delta\nu}{(B_e^{\text{BO}})^2}\left(\frac{Z_A}{M_A^2}+\frac{Z_B}{M_B^2}-\frac{g_J}{\mu m_p}\right), \tag{7}$$

where $\Delta\nu$ is the energy difference between the electronic ground state and the first excited states $\Omega=1$ of the same parity as the ground state, and Z_A and Z_B are the nuclear charges of atoms A and B, respectively. From this expression $\Delta_{01}^{\text{ad}} \lesssim -0.32$. The wobble-stretch theory predicts the correct order of magnitude of Δ_{01}^{ad} for different atoms,[53] but it cannot explain the anomalous value we obtained for $(\Delta_{01}^{\text{Si}})^{\text{ad}}$.

From U_{01} it is possible to calculate the so-called "Born–Oppenheimer" bond lengths r_e^{BO} (see Table VII), isotopically invariant since they are derived from a mass-independent parameter. r_e^{BO} for SiS is slightly larger than the previous value[41,53] owing to the new microwave data used in the fit.

The adiabatic bond lengths r^{ad} can also be calculated from our data using the relation

$$r^{\text{ad}} = r_e\left(1-\frac{\Delta Y_{01}^{(\text{D})}}{2B_e}-\frac{m_e g_J}{2m_p}\right)^{-1}. \tag{8}$$

These bond lengths are isotopically dependent and would correspond to the minimum of the adiabatic potential—the Born–Oppenheimer potential plus the adiabatic correction.[54] They are thus very similar to the r_e^{BO}'s (see Table VII).

B. Vibrational dependence of spin–rotation constants

The measurement of magnetic hfs in highly excited vibrational states is an interesting by-product of the present work. For the ^{29}Si isotopic species of SiO and SiS, the spin–rotation constant C_I was determined up to $v=26$ and 29, respectively, which provides information on the molecular electronic distribution that is otherwise not readily available for a molecule with a $^1\Sigma^+$ electronic ground state and no hfs in the absence of molecular rotation.

Nuclear spin–rotation depends on the molecular magnetic field, which arises from the rotation of the nuclear charges and from the rotation-induced second-order interaction of excited electronic states having nonzero orbital angular momentum with the ground electronic state. For a diatomic molecule these two contributions are usually expressed as:[56]

$$\begin{aligned} C_I &= C_I^{\text{nucl}} + C_I^{\text{el}} \\ &= -\frac{2e\mu_N g_I B}{\hbar c}\frac{Z_l}{R} - \frac{2e\mu_N g_I B}{\hbar c m} \\ &\quad \times \sum_k \frac{\langle 0|L_x|k\rangle\langle k|L_x r^{-3}|0\rangle + \langle 0|L_x r^{-3}|k\rangle\langle k|L_x|0\rangle}{E_0 - E_k}, \end{aligned} \tag{9}$$

where e and m are the charge (positive) and the mass of the electron, respectively, μ_N is the nuclear magneton, g_I is the nuclear g factor of the ith nucleus, B is the rotational constant, R the internuclear distance, Z_l the atomic number of the other nucleus in the diatomic molecule, and $\langle 0|$ and $|k\rangle$ designate the ground and excited electronic states.

The rotational constant is expected to decrease with increasing vibrational excitation. However, the magnetic and dipole moments, and the efficiency of the excitation of the valence electrons in higher vibrational levels[57] also change with v. Because the relative contributions of these several effects are somewhat difficult to predict, the variation of C_I with v is not readily determined. Contradictory results have been obtained: the spin–rotation constant for the fluorine atom decreases in absolute value with vibrational quantum number in BrF and IF, while it increases in HF.[56]

To our surprise, our hyperfine measurements indicate that C_I is independent of the vibrational excitation for both ^{29}SiO and ^{29}SiS. The contribution of C_I^{nucl}, however, has been evaluated for both diatomics and found to decrease by $\sim$25%, from 1.93 kHz for $v=0$ to 1.44 kHz for $v=26$ in ^{29}SiO, while in ^{29}SiS it decreases by $\sim$20%, from 1.26 kHz for $v=0$ to 1.00 kHz for $v=29$. Since C_I is of the order of 10–20 kHz, it is clear that the electronic contribution to C_I is dominant.

C_I^{el} also varies with vibrational quantum number, decreasing in absolute value by $\sim$2% from $v=0$ to $v=26$ for ^{29}SiO and $v=29$ for ^{29}SiS, counteracting the change in C_I^{nucl}. Variations in C_I^{el} are affected by the change in the rotational constants B, which decreases with vibrational quantum number. However, C_I^{el}/B increases by $\sim$19% for ^{29}SiO and by $\sim$14% for ^{29}SiS from the ground vibrational state to the highest vibrational level detected, so the change in B alone does not explain the C_I^{el} variation.

To properly evaluate the vibrational dependence of the spin–rotation constants, it is necessary to include vibrational and centrifugal distortion effects,[58] which are neglected in the usual theoretical treatment of the spin–rotation [Eq. (4) results from averaging over the ground vibrational state with the nuclei at the equilibrium distance]. The complete expression for the spin–rotation constant of a nucleus i in a diatomic molecule valid at any internuclear distance is[58]

$$\begin{aligned} C_I &= C_I^{\text{nucl}} + C_I^{\text{el}} + C_I^{\text{acc}} \\ &= -\frac{e^2 g_I B}{Mc^2}\frac{Z_l}{R} - \frac{2e^2\hbar^2 g_I B}{\hbar M m c^2} \\ &\quad \times \sum_k \frac{\langle 0|\Sigma_n (l_{in})_x r_{in}^{-3}|k\rangle\langle k|\Sigma_n (l_{in})_x|0\rangle}{E_0 - E_k} + \frac{B}{c^2}\ddot{R}_{0i}R_{0i}, \end{aligned} \tag{10}$$

where r_{in} and l_{in} are the position and angular momentum of electron n relative to nucleus i, M is the proton mass, and C_I^{acc} is a relativistic correction arising from the acceleration of the nuclei, expressed in terms of R_{0i}, the distance of the nucleus i from the molecular center of mass, and $\ddot{R}_{0i}$, its second time derivative. The increase in C_I^{el}/B along the vibrational ladder derived above for both ^{29}SiO and ^{29}SiS is in fact the variation with vibrational quantum number (and hence with internuclear distance) of $\ddot{R}_{0i}R_{0i}$ and the sum in C_I^{el}.

C_I^{acc} for the nucleus i can be calculated for each vibration–rotation state vJ using the Dunham potential for $J=0$ as[58]

$$\langle C_I^{\mathrm{acc}}\rangle_{v,J} = + \frac{hm_l}{2m_i(m_i+m_l)} \times\left[2\left(v+\frac{1}{2}\right)B_e\omega_e - 4J(J+1)B_e^2\right], \qquad (11)$$

where m_i and m_l are the masses of the nuclei of the diatomic molecule. From this expression C_I^{acc} for ^{29}SiO and ^{29}SiS increases by roughly two orders of magnitude with v, but even for the highest vibrational states the C_I^{acc} values are of the order of Hz or smaller, 10^3 to 10^4 times smaller than C_I^{el}. Therefore, in ^{29}SiO and ^{29}SiS the increase in $(C_I^{\mathrm{el}}+C_I^{\mathrm{acc}})/\mathrm{B}$ with v arises from the interaction of the excited electronic states and the ground state, where the contribution of C_I^{acc} is negligible.

Because the nuclear spin–rotation constant and paramagnetic shielding are closely related quantities, vibrational and centrifugal distortion contributions are important to obtain magnetic shielding constants for the nonvibrating molecule at the equilibrium internuclear distance and to estimate with these NMR chemical shifts. Corrections for vibrational and centrifugal distortion effects are especially significant if comparisons are to be made between isotopic species of the same compound.

C. Vibrational relaxation

Excited vibrational states have been detected to as high as 71% of the dissociation limit in SO, 66% in SiO, and 61% in SiS. It is worth noting that the highest vibrational levels observed here for $X\,^3\Sigma^-$ and $b\,^1\Sigma^+$ of SO have approximately the same energy above ground. For the three diatomics here, even when a large fraction of the potential well has been sampled, no steep decrease in the intensity of the rotational transitions within the highest vibrational levels was observed, which suggests that VT exchange is still less important than VV energy transfer. Detection of yet higher vibrational states, closer to the dissociation limit, is probably required to observe the Boltzmann region predicted by theoretical models.[46]

The close similarity of the vibrational distribution in our molecular beam and that in the glow discharge of Ref. 22 is strong evidence of the predominance of VV energy transfer when the vibrational levels are very strongly excited, as in an electric discharge. This similarity also indicates that the electron temperature achieved in the two discharges is about the same. The VT exchange between the diatomic molecules and the atomic buffer gas in the molecular beam is clearly too slow to dissipate the energy excess via the lowest vibrational energy levels on the time scale of the experiment, and this fairly slow deactivation mechanism is overcome by the much more rapid VV exchange. Because VV transfer is so important in determining the vibrational temperature, it is not surprising that no significant change is observed when He is used instead of Ne as the carrier gas. The slight difference may result from differences in ionization efficiencies [4.6×10^{-2} for He versus 5.6×10^{-2} for Ne (Ref. 44)] or ionization potentials (24.6 eV versus 21.6 eV[59]).

Relaxation of molecular vibration depends on the number of binary collisions in the supersonic expansion and on the vibrational frequencies, the high-frequency vibrations generally requiring many more collisions than the low ones for relaxation to occur. The total number of binary collisions in the throat of the supersonic expansion ($\sim10^2$–10^3 collisions) is below the number required to relax the vibrational modes of most diatomic molecules, such as those studied here. It would be useful to examine how varying the backing pressure and hence the collision rate downstream changes the vibrational distribution. For alkali halides[14,15] and I_2,[16,17] the vibrational relaxation increases with pressure for $v\leqslant5$ in the absence of an electric discharge. Similar investigations for diatomic molecules in a molecular beam discharge source like that here might allow changes in vibrational populations to be observed over many levels.

The three diatomics here possess vibrational modes with fundamentals far above kT (T being $\approx$300 K, the temperature behind the nozzle) and similar vibrational temperatures. For NO, with $\omega_e=1904.2\ \mathrm{cm}^{-1}$,[29] a vibrational temperature of 6700 ± 700 K for $v=6$–18 has been derived[19] after applying an electric discharge of 1150 V to a supersonic expansion of 5% NO in He at 2.25 kTorr, in excellent agreement with our results. Investigations of diatomics with vibrational frequencies around or below kT will be desirable to test the validity of the proposed model for those molecules. Among them, I_2 has a vibrational frequency only slightly above kT [$\omega_e=214.5\ \mathrm{cm}^{-1}$ (Ref. 29)] and its vibrational relaxation in a molecular beam after laser pumping to an electronically excited state has been investigated under various conditions.[16,17] Vibrational temperatures were only derived for the $v=0$–3 vibrational states of the ground electronic state, and these were found to be considerably lower (150–240 K for monoatomic diluents) than those derived in this work at low v—a possible indication that VT energy transfer is much more efficient in this molecule.

SO, SiO, and SiS are important astrophysical molecules. SO is widely distributed in galactic molecular clouds and has also been detected in the cores of star-forming regions (see Ref. 23, and references therein). It is claimed that shock waves associated with star formation may form SO in highly excited states. SiO is well known astronomically as a source of highly compact and intense maser emission. Maser and nonmaser emission transitions from SiO, for the normal and rare isotopic species and in the ground as well as in excited vibrational states, have been used to probe physical and chemical conditions in space (see Ref. 37, and references

therein). SiS has been detected in several astronomical sources,[60–62] and it is believed to play an important role in the photodissociation chemistry of the rich circumstellar envelope of IRC+10216,[39,40] where rotational transitions of SiS in the $v=1$ excited vibrational state have been observed.[63] Vibrationally excited states will be populated in space in sources with high temperatures or where collisions with electrons are important. Precise microwave frequencies for the rotational lines of many excited vibrational levels of these three diatomic molecules are provided here, and from these measurements and the derived molecular constants, transitions in the range of interest to radioastronomers can be calculated to the required accuracy (i.e., better than 1 ppm) to conduct precise astronomical searches.

Note added in proof. We recently became aware that Kim and Yamamoto [J. Mol. Spectrosc. **219**, 296 (2003)] in a parallel work detected SO in the *b* electronic state up to $v=22$. Their results agree well with those presented here.

ACKNOWLEDGMENTS

The authors wish to thank P. Bernath for providing IR frequencies for SiO and SiS, and R. L. LeRoy and C. A. Gottlieb for comments and advice. This work has been supported by NASA Grant NAG5-9379 and NSF Grant AST-9820722. M.E.S. gratefully acknowledges an FPI postdoctoral grant from the Secretaría de Estado de Educación, Universidades, Investigación y Desarrollo (Ministerio de Educación, Cultura y Deporte, Spain).

[1] A. C. Legon, in *Atomic and Molecular Beam Methods*, edited by G. Scoles (Oxford University Press, Oxford, 1992), Vol. 2, Chap. 9.
[2] Y. Endo, H. Kohguchi, and Y. Ohshima, Faraday Discuss. **97**, 341 (1994).
[3] K. A. Walker, C. J. Evans, S.-H. K. Suh, M. C. L. Gerry, and J. K. G. Watson, J. Mol. Spectrosc. **209**, 178 (2001), and references therein.
[4] P. Thaddeus and M. C. McCarthy, Spectrochim. Acta, Part A **57**, 757 (2001).
[5] Y. Ohshima and Y. Endo, Chem. Phys. Lett. **256**, 635 (1996).
[6] C. A. Gottlieb, A. J. Apponi, M. C. McCarthy, P. Thaddeus, and H. Linnartz, J. Chem. Phys. **113**, 1910 (2000).
[7] V. D. Gordon, E. S. Nathan, A. J. Apponi, M. C. McCarthy, P. Thaddeus, and P. Botschwina, J. Chem. Phys. **113**, 5311 (2000).
[8] P. Botschwina, M. E. Sanz, M. C. McCarthy, and P. Thaddeus, J. Chem. Phys. **116**, 10719 (2002).
[9] M. E. Sanz, M. C. McCarthy, and P. Thaddeus (unpublished).
[10] M. Cacciatore, M. Capitelli, S. De Benedictis, M. Dilonardo, and C. Gorse, Topics in Current Physics **39**, 5 (1986); M. Capitelli, C. Gorse, and A. Ricard, *ibid.* **39**, 315 (1986).
[11] R. Farrenq, C. Rossetti, G. Guelachvili, and W. Urban, Chem. Phys. **92**, 389 (1985); R. Farrenq and C. Rossetti, *ibid.* **92**, 401 (1985).
[12] S. De Benedictis, G. Dilecce, and M. Simek, J. Chem. Phys. **110**, 2947 (1999).
[13] I. Kimura, JSME Int. J., Ser. II **31**, 376 (1988).
[14] R. P. Mariella, Jr., S. K. Neoh, D. R. Herschbach, and W. Klemperer, J. Chem. Phys. **67**, 2981 (1977).
[15] H. G. Bennewitz and G. Buess, Chem. Phys. **28**, 175 (1978).
[16] G. M. McClelland, K. L. Saenger, J. J. Valentini, and D. R. Herschbach, J. Phys. Chem. **83**, 947 (1979).
[17] A. Amirav, U. Even, and J. Jortner, Chem. Phys. **51**, 31 (1980).
[18] J. Fleniken, Y. Kim, and H. Meyer, Chem. Phys. Lett. **318**, 529 (2000).
[19] G. B. Courrèges-Lacoste, J. P. Sprengers, J. Bulthuis, S. Stolte, T. Motylewski, and H. Linnartz, Chem. Phys. Lett. **335**, 209 (2001).
[20] J.-U. Grabow, S. Palmer, M. C. McCarthy, and P. Thaddeus (unpublished).
[21] M. C. McCarthy, W. Chen, M. J. Travers, and P. Thaddeus, Astrophys. J., Suppl. Ser. **129**, 611 (2000).
[22] R. Mollaaghababa, C. A. Gottlieb, J. M. Vrtilek, and P. Thaddeus, Astrophys. J. Lett. **368**, L19 (1991).
[23] M. Bogey, S. Civiš, B. Delcroix, C. Demuynck, A. F. Krupnov, J. Quiguer, M. Y. Tretyakov, and A. Walters, J. Mol. Spectrosc. **182**, 85 (1997).
[24] J.-U. Grabow, N. Heineking, and W. Stahl, Z. Naturforsch. A **46A**, 914 (1991).
[25] F. J. Lovas, R. D. Suenram, T. Ogata, and S. Yamamoto, Astrophys. J. **399**, 325 (1992).
[26] N. Hansen, U. Andresen, H. Dreizler, J.-U. Grabow, H. Mäder, and F. Temps, Chem. Phys. Lett. **289**, 311 (1998).
[27] Th. Klaus, A. H. Saleck, S. P. Belov, G. Winnewisser, Y. Hirahara, M. Hayashi, E. Kagi, and K. Kawaguchi, J. Mol. Spectrosc. **180**, 197 (1996).
[28] See EPAPS Document No. E-JCPSA6-119-96340 for seven tables with the frequencies of the measured rotational transitions of $X\ ^3\Sigma^-$ SO, $X\ ^3\Sigma^-\ ^{33}$SO, $b\ ^1\Sigma^+$ SO, SiO, ^{29}SiO, SiS, Si^{34}S, and ^{29}SiS. A direct link to this document may be found in the online article's HTML reference section. The document may also be reached via the EPAPS homepage (http://www.aip.org/pubservs/epaps.html) or from ftp.aip.org in the directory /epaps/. See the EPAPS homepage for more information.
[29] K. P. Huber and G. Herzberg, *Molecular Spectra and Molecular Structure*, Vol. IV, Constants of Diatomic Molecules (Van Nostrand Reinhold, New York, 1979).
[30] S. Yamamoto, Chem. Phys. Lett. **212**, 113 (1993).
[31] R. J. LeRoy, DSPARFIT 2.0: *A Computer Program for Fitting Multi-Isotopomer Diatomic Molecule Spectra* (University of Waterloo Chemical Physics Research Report CP-653, 2001). http://leroy.uwaterloo.ca
[32] R. J. LeRoy, J. Mol. Spectrosc. **194**, 189 (1999).
[33] T. Törring, Z. Naturforsch. A **23**, 777 (1968).
[34] E. L. Manson, Jr., W. W. Clark, F. C. De Lucia, and W. Gordy, Phys. Rev. A **15**, 223 (1977).
[35] J. W. Raymonda, J. S. Muenter, and W. A. Klemperer, J. Chem. Phys. **52**, 3458 (1970).
[36] J. M. Campbell, D. Klapstein, M. Dulick, P. F. Bernath, and L. Wallace, Astrophys. J., Suppl. Ser. **101**, 237 (1995).
[37] S.-H. Cho and S. Saito, Astrophys. J. Lett. **496**, L51 (1998).
[38] H. M. Pickett, J. Mol. Spectrosc. **148**, 371 (1991).
[39] D. A. Howe and T. J. Millar, Mon. Not. R. Astron. Soc. **244**, 444 (1990).
[40] A. E. Glassgold and G. A. Mamon, *Chemistry and Spectroscopy of Interstellar Molecules*, edited by D. K. Bohme, E. Herbst, N. Kaifu, and S. Saito (University of Tokyo Press, Tokyo, 1992), pp. 261–266.
[41] C. I. Frum, R. Engleman, Jr., and P. F. Bernath, J. Chem. Phys. **93**, 5457 (1990).
[42] E. Tiemann, J. Phys. Chem. Ref. Data **5**, 1147 (1976).
[43] G. Maroulis, C. Makris, D. Xenides, and P. Karamanis, Mol. Phys. **98**, 481 (2000).
[44] A. von Engel, *Ionized Gases* (American Institute of Physics, New York, 1994), p. 63.
[45] D. R. Miller in *Atomic and Molecular Beam Methods*, edited by G. Scoles (Oxford University Press, New York, 1988), Vol. 1, Chap. 2.
[46] S. H. Lam, J. Chem. Phys. **67**, 2577 (1977).
[47] C. E. Treanor, J. W. Rich, and R. G. Rehm, J. Chem. Phys. **48**, 1798 (1968).
[48] W. W. Clark III and F. C. De Lucia, J. Chem. Phys. **74**, 3139 (1981).
[49] J. Wildt, E. H. Fink, R. Winter, and F. Zabel, Chem. Phys. **80**, 167 (1983).
[50] A. C. Borin and F. R. Ornellas, Chem. Phys. **247**, 351 (1999).
[51] S. Saito, J. Chem. Phys. **53**, 2544 (1970).
[52] E. Tiemann, H. Arnst, W. U. Stieda, T. Törring, and J. Hoeft, Chem. Phys. **67**, 133 (1982).
[53] N. Authier, N. Bagland, and A. Le Floch, J. Mol. Spectrosc. **160**, 590 (1993).
[54] J. K. G. Watson, J. Mol. Spectrosc. **45**, 99 (1973).
[55] B. Rosenblum, A. H. Nethercot, Jr., and C. H. Townes, Phys. Rev. **109**, 400 (1958).
[56] H. S. P. Müller and M. C. L. Gerry, J. Chem. Phys. **103**, 577 (1995).
[57] S. M. Bass, R. L. DeLeon, and J. S. Muenter, J. Chem. Phys. **86**, 4305 (1987).
[58] N. F. Ramsey, Phys. Rev. **87**, 1075 (1952); **90**, 232 (1953); D. K. Hindermann and C. D. Cornwell, J. Chem. Phys. **48**, 4148 (1968).
[59] *CRC Handbook of Chemistry and Physics*, 3rd Electronic ed. (CRC, Boca Raton, 2001), pp. 10–175.
[60] M. Morris, W. Gilmore, P. Palmer, B. E. Turner, and B. Zuckerman, Astrophys. J. Lett. **199**, L47 (1975).
[61] W. Aoki, T. Tsuji, and K. Ohnaka, Astron. Astrophys. **340**, 222 (1998).
[62] R. Lucas, M. Guélin, C. Kahane, P. Audinos, and J. Cernicharo, Astrophys. Space Sci. **224**, 293 (1995).
[63] B. E. Turner, Astron. Astrophys. **183**, L23 (1987).